Advances in Decommissioning Using Laser Cutting – 16035

Paul Hilton[*], Daniel Lloyd[**], Nick Ellis[***]
[*]TWI Ltd
[**]Laser Optical Engineering
[***]ULO Optics Ltd

ABSTRACT

This paper describes advancements made in laser cutting in the UK Collaborative Project 'LaserSnake2'. In particular it will focus on the use of special laser cutting heads and optics to enhance cutting performance, whilst at the same time, reducing the effects of the residual laser beam passing through the cut. The benefits of using lasers for applications in decommissioning include the high speeds available, the tolerance of the process, the lightness of the cutting head, the lack of a reaction force with the part being cut and the ease of automation of the laser cutting operation. Laser cutting, however, is a thermal process and a potential detriment, is that the residual laser beam passing through the kerf, might damage or indeed set fire to, something positioned behind the part being cut. This paper describes the use of a diffractive optical element in the laser beam forming optics, designed to extend the depth of focus of the system, without increasing the physical focal length of the optic. In this way, for cutting thick materials, the goal is to achieve the cutting performance of a long focal length lens, with the beam divergence of a short focal length lens. A design of diffractive optical element is presented, which when used with a laser power of 5kW, in conjunction with a set of conventional beam forming optics, including a 250mm focal length focusing lens, is able to cut 40mm thick C-Mn steel plate at 50mm/min, while varying the nozzle tip to plate stand-off distance by 100mm. For the same laser power in the focusing beam, this performance can be equaled by removing the diffractive optic and 250mm lens and replacing these with just a 500mm lens. However, when using the diffractive optical element, the power density in the residual beam has been reduced by a factor four when compared to that from the optical arrangement using the 500mm lens. As well as the cutting performance, the effect of the two different power density residual beams on concrete will be presented.

INTRODUCTION

Since 2009, TWI Ltd. and others have demonstrated the potential of laser cutting for size reduction in nuclear decommissioning. [1-5]. In 2014, TWI used a 5kW fibre laser to size reduce radioactive Magnox type waste containers at a nuclear licensed site in the UK, [6]. Although the papers cited above demonstrate the benefits of laser cutting, such as ease of automation, high process speeds and lack of reaction force from the cutting tool on the material being cut, from the nuclear safety case point of view, there are some drawbacks to using laser beams for cutting. These include, but are not limited to, the effects of 'stray' beams that pass through the material being cut and impinge on something behind the cutting point, the temperature rise in the material being cut and the effects of the sparks generated in the laser cutting process. In addition, the amount of material removed from the cut kerf (hereafter in this paper referred to as dross), and fume generated and how this is dealt with, are also of

concern. Hilton, [7] has addressed some of the safety case aspects described above, in particular the results, in terms of induced temperature rise and damage, of 'stray' laser beams of various power densities, impinging, either when stationary or when moving, on materials such as concrete, graphite and C-Mn and stainless steel.

From these results it can be seen that the incident laser power density plays an important role in terms of both induced damage and temperature rise. For a given delivery fibre diameter and collimating lens, the residual power density in the beam will depend on the focal length of the beam focusing optic. A longer focal length will produce a greater Raleigh length, benefiting the cutting of thick materials but it will also produce a higher power density in the beam passing through the focus. In order to address this limitation of conventional refractive optics for forming the beam, the use of diffractive optical elements (DOE's), which can be used to generate complex two and three dimensional energy distributions, has been investigated. DOE's are widely used with low power lasers, generally in the visible part of the spectrum, for applications such as optical interconnects, multiple focusing and image processing. However, their effective use in high power laser applications has been limited to date. A number of authors [8-9] have described various reflective diffractive optics for use with carbon dioxide laser sources. The resulting beams were used in applications involving the soldering of several asymmetrically positioned joints on a circuit board, to the simultaneous welding and cutting of plastic foils. It has also been shown [10] that it is possible to manage the melt flow in a weld pool by the use of a diffractive optic, through a redistribution of the incident energy distribution, in both spatial and power terms. Olsen [11] has described the application of tailored beam patterns to laser cutting.

This paper describes the use of a transmissive DOE in the laser beam forming optics, designed to extend the depth of focus of the system, without increasing the focal length of the focusing optic. In this way, for cutting thick materials, the goal is to achieve the cutting performance of a long focal length lens, whilst maintaining the beam divergence of a short focal length lens. A design of DOE is described which, when used with the beam from a 1µm wavelength high power fibre laser, in conjunction with a 250mm focal length focusing lens, was able to cut 40mm thick C-Mn steel plate at a travel speed of 50mm/min, whilst varying the nozzle tip to plate stand-off distance by as much as 100mm. For comparison purposes and using the same laser power in the focusing beam, the cutting performance of a 500mm focusing lens alone was also established.

SPECIFICATION, MANUFACTURE AND TESTING OF THE DOE

DOE's use computer generated holographic patterns, which when illuminated with coherent radiation diffract that energy into a mathematically specified distribution. A number of mathematical models are available for the computer generation of a holographic pattern and for the method by which the light is redistributed [12,13]. A DOE consists of an array of apertures, which diffract the incident beam. The transmitted beam propagates from each of these pixels and the desired beam shape is created in the image plane, through use of constructive and destructive interference. Two designs of DOE can be considered. In a 'shaper' DOE, the algorithms are optimised to diffract the incident light through as small an angle as possible. The

alternative ‘diffuser' type DOE, operates slightly differently, in that the input beam is scattered across the output image, meaning that there is more design freedom, allowing potentially higher efficiencies and typically, resulting in larger diffraction angles. The DOE produced for this work is a ‘diffuser’ type, which is considered to be more tolerant to variations in the input beam than a ‘shaper’ type. This is advantageous when the exact mode of the beam may change, as is the case for the high powered multimode laser used in this work.

The design of the DOE was undertaken by considering the input beam and the requirements of the desired beam shape in the image plane. This determined both the size of the hologram on the DOE and of each aperture within it. An iterative Fourier transform algorithm was then used to calculate the hologram. In this case, a kinoform (a hologram that only operates on the phase of the beam) was used, in order to reduce the computational power required and also to simplify the manufacturing process. The algorithm iteratively propagated the image beam backwards to the hologram plane, until the resulting output matched the required design. In this case the desired beam shape was a ‘top hat’ distribution, with a diameter of 0.6mm at the beam waist and an extended depth of focus, compared to a conventional beam. This condition was met by additionally introducing a 250mm standard focusing lens below the DOE. The use of a separate focusing element means that the DOE could be utilised with different conventional focusing lenses to generate alternative energy distributions.

The resulting kinoform is represented by a greyscale image, such as the one shown in Figure 1, where each pixel forms an aperture of the final hologram. The depth of colour of the pixel represents the relative height of the aperture or the phase change which generates the beam. In this case the individual pixels represent square apertures which have side lengths of 112 µm. The maximum pixel height of 2.4µm was calculated as a function of the wavelength and refractive index of the substrate material of the DOE. The positioning of each aperture in three dimensions is critical to good optical performance. The kinoform shown in Figure 1 was plasma etched into a fused silica window in a single process, producing a transmissive DOE in a relatively fast manufacturing time. The final holographic element contained 32 step heights, allowing a diffractive efficiency (related to the amount of incident light transmitted) of over 92%.

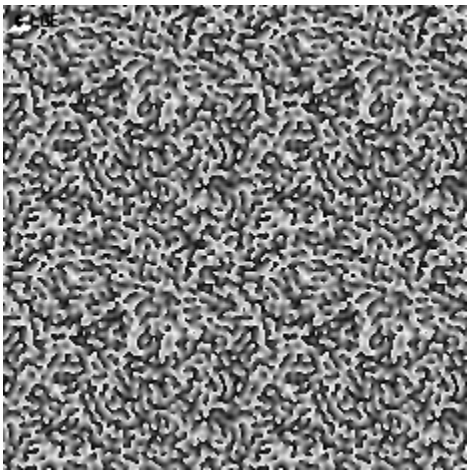

Figure 1. *Holographic kinoform design.*

The DOE used for this testing was designed to be used in conjunction with a separate focusing lens, (rather than including a Fresnel focusing function in a single optical element). The addition of an extra lens increases the transmissive losses due to the increased number of surfaces, anti-reflection coatings for the laser wavelength were not applied to this DOE which also reduced the transmissive efficiency compared to optics typically used for laser processing. Despite this, tests showed that the transmitted power loss was comparable to that of a conventional uncoated optic and the DOE proved to be stable under illumination, at up to 5kW applied power, for extended diagnostic and cutting trials. Improved optical efficiency could be obtained by use of such coatings. In addition, some power loss is present within the noise terms of the output image as result of the kinoform having less than 100% diffraction efficiency.

In this work, a Prometec Laserscope UFF 100 was used to measure laser beam profiles of the caustics produced, using the well reported mechanical scanning technique, whereby a needle is rapidly scanned across the laser beam. The needle has a small pinhole drilled near its end, which, since its aperture is smaller than the diameter of the laser beam, only samples a fraction of the beam at any one time. The high scan speed ensures that there is a short interaction time between the laser beam and the needle, eliminating heating effects. A mirror situated at the bottom of the needle reflects the sampled beam to a detector. The power intensity distribution is measured by recording a cross-section of the beam as the needle is scanned through it, which allows various characteristics of the laser beam at that cross-section (i.e. single plane) to be determined. Measuring the power intensity distribution at different positions, along the direction of the laser beam propagation, allows a beam caustic to be calculated. Hyperbolic functions can be fitted to the measured profiles allowing the beam caustic and a number of calculated values to be generated.

Three optical configurations (250mm focusing lens alone, 500mm focusing lens alone and DOE plus 250mm focusing lens), were used in testing and the resulting beam profiles at focus can be seen in Figure 2. For the two conventionally focused profiles (left and centre), these closely resemble the expected ‘top hat’ intensity profile, imaging the end of the optical delivery fibre used. As can be seen from the beam profile for the combination of DOE and 250mm lens (right), the beam diameter is similar to that of the 500mm lens alone but the intensity profile at the beam waist is less ‘top hat’. Due to the unknown mode distribution of the fibre laser used in this work, effort was primarily directed into extending the focal depth achievable by use of the DOE. As a result, the intended ‘top hat’ energy distribution has not been effectively reproduced.

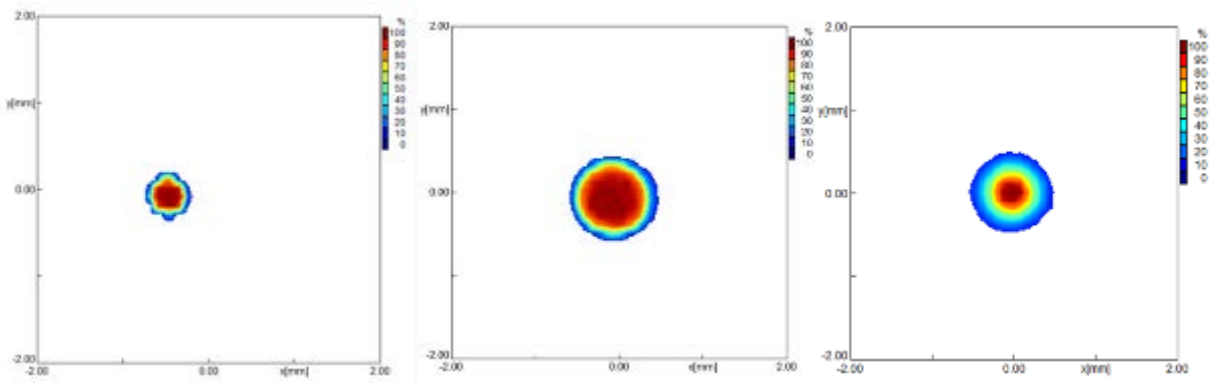

Figure 2. *Intensity profiles at the beam waist positions for (left) 250mm, lens, (centre) 500 mm lens and (right) DOE plus 250mm lens. All axes are 4mm long.*

In addition to the measurements in the focal plane, beam caustics were also produced for the above optical configurations. Key calculated parameters are given in Table 1 and the resulting 3D plots are presented in Figure 3.

From Table 1 and Figure 3 it can be seen that the DOE and 250mm lens combination has significantly increased the Rayleigh length and effective focal depth of the laser beam, when compared to the results for the 250mm lens alone. It has also significantly increased the M2 value, compared to that of the conventional beams, largely resulting from the increased diameters. The waist diameter of the DOE produced beam is slightly larger than defined in the original calculation and this is believed to be because the raw beam profile was more uniform than anticipated and so the assumed input for the design was closer to Gaussian than was actually the case. The measured Rayleigh length of the DOE and the 250mm lens was approximately twice that of the 250mm lens alone and half that of the 500mm lens alone.

	Units	250 lens alone	500 lens alone	250 lens plus DOE
Beam waist radius, wO (r86%)	mm	0.17	0.38	0.43
Rayleigh length zR (r86%)	mm	6.39	25.53	13.88
Time limit diffraction factor M^2 (r86%)		13.81	17.14	39.45
Waist area (r86%)	mm^2	0.09	0.46	0.58
Power density at 5kW	kW/mm^2	53.17	10.79	8.61

Table 1. *Beam parameters as calculated by the Prolas software according to DIN EN ISO 11146.*

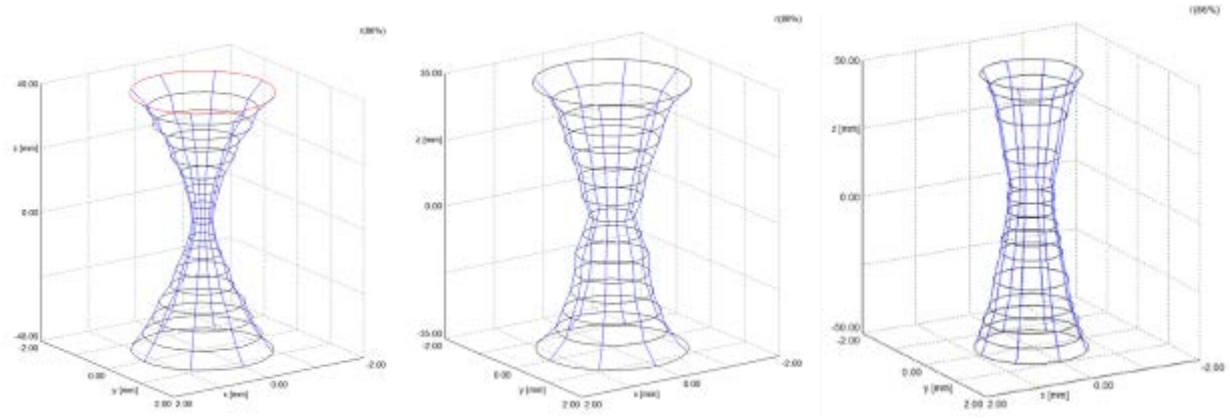

Figure 3. *Caustics for 250mm lens (left), DOE and 250mm lens (centre), and 500mm lens (right). The vertical ranges in these plots are +/- 40mm, 35mm and 50mm respectively, with each lateral axis being 2mm long.*

EXPERIMENTAL ARRANGEMENTS

The laser cutting system used for these experiments consisted of a 10kW industrial fibre laser, (emitting laser light at a wavelength close to 1µm), a delivery fibre of core diameter 200 µm, a collimating lens of 120mm focal length and focusing lenses of 250mm and 500mm focal length. The DOE described above, when in use, was positioned in the optical system, just above the 250mm focusing lens. The cutting nozzle tip had an exit diameter of 3mm and for all three optical arrangements tested (250mm lens alone, 250mm lens plus DOE and 500mm lens alone), the beam waist was always located 25mm below the nozzle tip. For all the experiments described, the cutting gas was compressed air at 8bar. (The use of oxygen as cutting gas in a nuclear environment would not be allowed due to the risk of explosion and as cut quality in this application is not a requirement, there is little point in the use of expensive inert gases). As the DOE did not have anti-reflective coatings, it was expected that the laser power measured below the optics would be different when the DOE was in the

optical train. As a result, before cutting experiments began, the laser settings were recorded which produced exactly 5kW of transmitted power through each of the three optical configurations used. The power after the optics was measured on a calibrated laser power meter, manufactured by Ophir. All subsequent laser cutting experiments were conducted with 5kW laser power incident on the material being cut, regardless of the optical system used. The materials for the cutting trials consisted of plates of S355J2+N C-Mn steel, of thicknesses 60 and 40mm.

PRELIMINARY CUTTING TRIALS

In this experiment a 60mm thick plate of C-Mn steel was used with its edge machined away at 45 degrees, so as to offer a range of thickness to the laser beam, as can be seen in Figure 4.

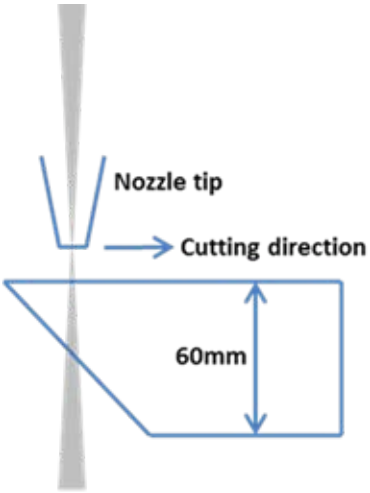

Figure 4. *Cutting geometry used in the preliminary experiments.*

The beam was traversed into the plate at various speeds, from 50mm/min to 1000mm/min, until it was clear that, at each speed, cutting had stopped. The maximum cut depth achieved was measured afterwards by examination of the sloping face, as can be seen in Figure 5. In this series of experiments, the cutting depth was established for each optical configuration, for three positions of the laser beam focus with respect to the material surface, viz -20mm (beam focus 20mm below the material surface, 0mm (beam focus on the material surface) and +20mm (beam focus 20mm above the material surface). As the nozzle tip to beam focus distance was always 25mm, this corresponded to nozzle to plate stand-off distances from 5mm to 45mm. The best cutting performance, in terms of depth achieved, was always seen at a focus position of -20mm, and the results for this position can be seen in Figure 6.

Figure 5. *Example showing depth of cut achieved for five different cutting speeds (note each speed was repeated three times and an average of the recorded depths taken).*

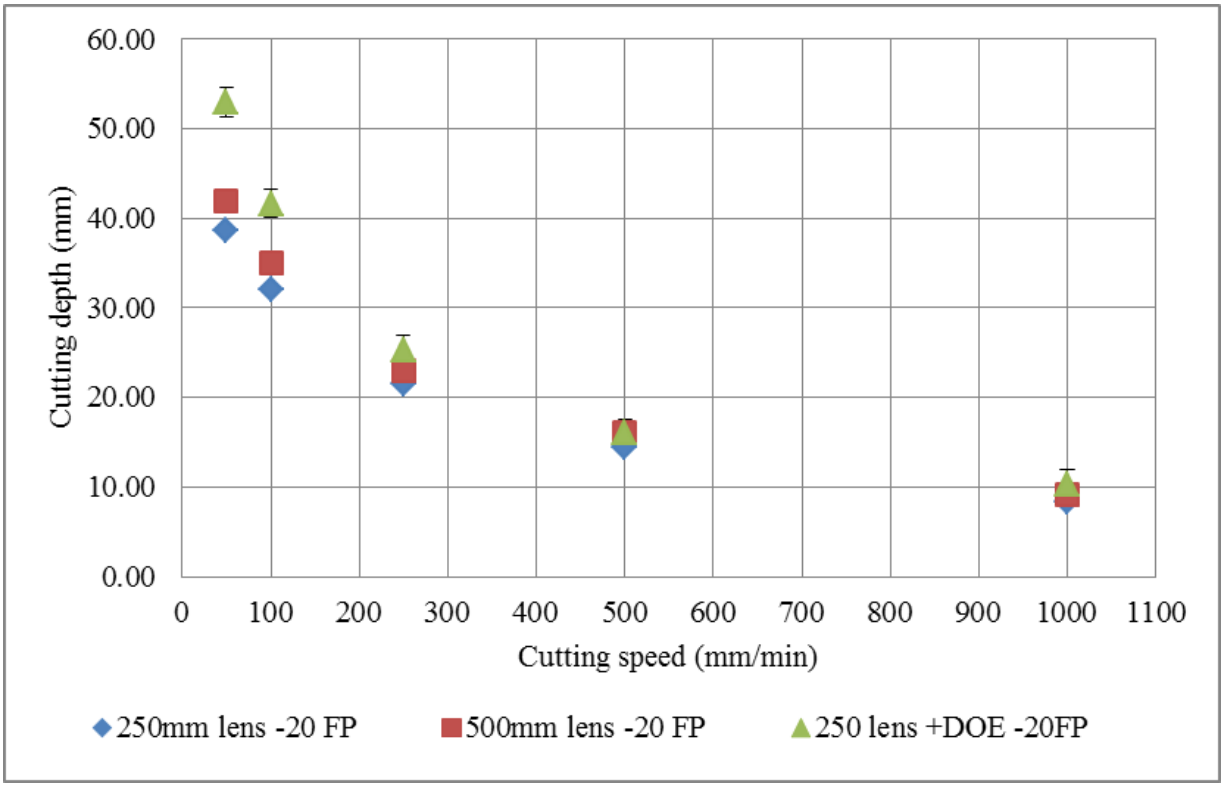

Figure 6. *Cutting depth achieved against travel speed on C-Mn steel. Laser power 5kW and beam focus position 20mm below material surface.*

Figure 6, indicates that at the high cutting speeds (lowest cutting depth), the performance of the three different optical configurations was essentially the same. However, at speeds below 100mm/min, differences appear. It is clear that at slow speeds the worst performer, in terms of cutting depth, was the 250mm lens alone. Slightly better was the 500mm lens alone, which might be expected as the cutting depth is now of the order 40mm. The best performance was seen from the combination of DOE and 250mm lens. Whilst the above method of using the wedge shaped sample provides a relatively fast and easy way of establishing cutting performance, the beam/material interactions are not exactly the same as when cutting plates of a given thickness and so further trials were undertaken on plate material of 40mm thickness.

CUTTING 40MM THICK C-MN STEEL PLATE

Because any practical application of laser cutting would have to be performed remotely, manipulating the cutting head in a robot arm or other such delivery

mechanism, it is important to establish the cutting tolerance to beam focus position (or stand-off distance). As a result, for the trials on 40mm thick material, focal positions from -20mm to +90mm were investigated (corresponding to stand-off distances from 5mm to 115mm). Again the laser power was constant at 5.0kW for all cuts and the cutting gas pressure was 8bar. Table 3 shows the maximum cutting speeds achieved to sever 40mm C-Mn steel plate. The maximum cutting speed is defined as the speed where, if the speed was incremented by 10mm/min, a cut was not achieved.

	Maximum cutting speed for 40mm thickness (mm/min)		
Focal position (mm)	**250 lens only**	**DOE and 250 lens**	**500 lens only**
-20	80	100	100
0	70	80	100
20	60	80	90
40	50	70	70
80	Did not cut	50	50

Table 3. *Maximum cutting speed on 40mm thick C-Mn steel at various positions of the beam focus.*

From Table 3 it can be seen that for cutting 40mm thick C-Mn steel at speeds between 50 and 100mm/min, the performance of the 500mm lens alone (over the wide range of focal positions) is only marginally better than that of the DOE and 250mm lens combination and both are better than the 250mm lens alone.

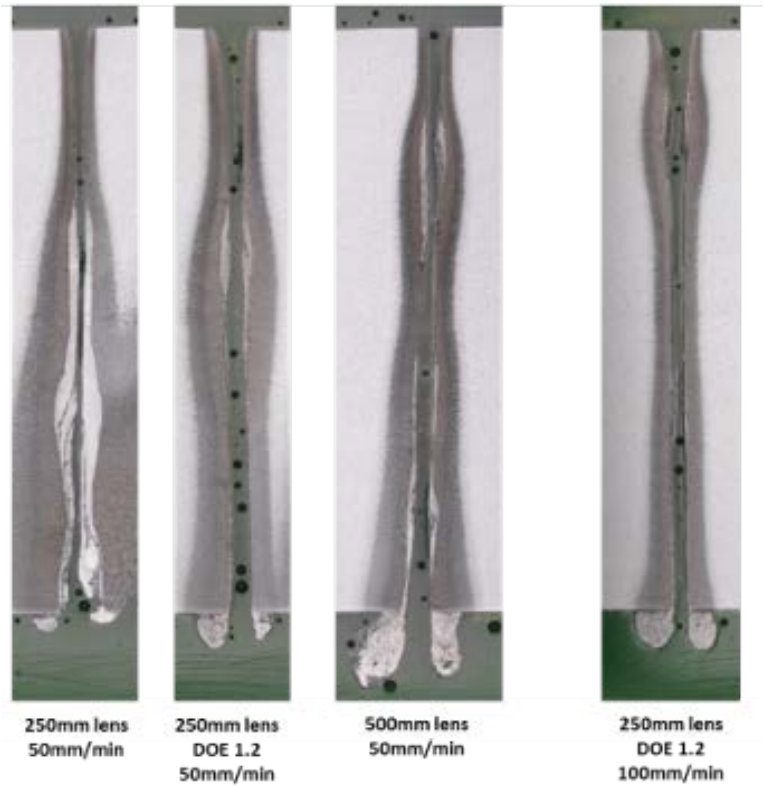

Figure 7. *Sections produced to show the form of the kerfs. The material thickness is 40mm in all cases*

Figure 7, shows sections prepared to show the kerf widths produced and the heat affected zones, corresponding to using the three optical configurations and cutting at 50mm/min. In addition, a kerf produced whilst cutting at 100mm/min and using the DOE, is also shown. In this figure the apparent porosity which can be seen in the kerfs, is in fact holes in the potting compound used to hold the samples during polishing.

Configuration	Focus position range covered	Equivalent stand-off range covered	Cutting speed possible
250mm lens alone	-20 to +40mm	60mm	50mm/min
500mm lens alone	-20 to +80mm	100mm	50mm/min
250mm lens + DOE	-20 to +80mm	100mm	50mm/min
250mm lens + DOE	-20 to +20mm	40mm	100mm/min

Table 4. *Stand-off tolerance and cutting speed for 40mm thick C-Mn steel.*

In order to demonstrate the tolerance to focus position, 40mm thick samples, 200mm long, were cut at speeds of either 50 or 100mm/min, where the cutting head was programmed to move up and down from a focus position of -20mm to a focus position well above the plate surface and back, twice, over the length of the sample. All other process parameters remained constant. Table 4 shows the speeds and focus position ranges obtained for the three focusing systems used. For all these conditions, extending the standoff distance range by 10mm, resulted in an incomplete cut. Figure 8, shows the cut face of one such sample, made using the DOE and the 250mm lens, at a speed of 50mm/min. Figure 9 shows the same for the 500mm lens alone, again at 50mm/min. As can be seen, the cut surfaces are similar but the striation pattern when using the DOE looks to be more complex than that from the 500mm lens alone. In these figures, the two positions where the cutting head was at its highest point above the material surface, corresponded to the two positions on the lower surface having the highest levels of adhering dross.

Figure 8. *Cut face from a 200mm long sample of C-Mn steel cut using the 250mm lens and the DOE.*

Figure 9. *Cut face from a 200mm long sample of C-Mn steel cut using the 500mm lens alone.*

Figure 10 shows the top view of the opposite side of the sample shown in Figure 8. What can be seen is the variation in kerf produced along the cut as the beam focus position changes.

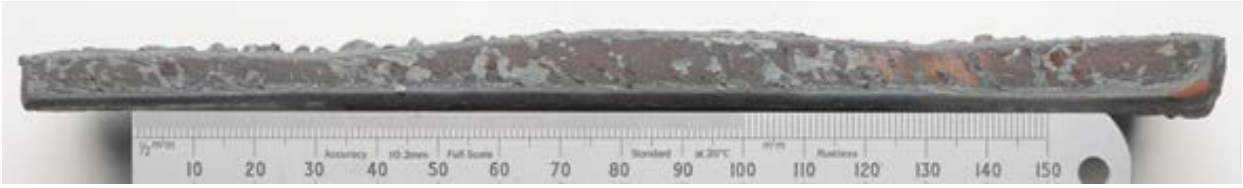

Figure 10. *Top view of opposite side of sample shown in Figure 8.*

Video of the cutting of these 40mm thick samples can be seen at https://youtu.be/2lHuaszpe-U

DISCUSSION

Whilst the DOE was intended to produce a 'top hat' energy distribution at the beam waist, this was not achieved, as can be seen from Figure 2. It is believed the multimode distribution of the fibre laser used has degraded the achievable resolution in the image plane, with the effect that the edge definition has been lost. While this was designed to be approximately 10% of the beam width, in reality, it is believed this figure could only be achieved by using a single mode laser. Nevertheless, the DOE has effectively doubled the beam waist diameter of the 250mm lens and increased the

Raleigh length.

The experimental work has shown that the cutting performance, in terms of tolerance to nozzle tip to plate distance, for cutting 40mm thick CMn steel, can be extended by the introduction of a diffractive optical element into the laser beam forming optics. This tolerance for the 250mm focusing lens alone, at a speed of 50mm/min, was from a beam focus position of -20mm to +40mm. Adding the DOE increased the stand-off tolerance range to -20mm to +80mm, at the same cutting speed. This performance was in fact very similar to that for the 500mm lens alone. As can be seen from Figure 11, there are significant implications for this in the case of cutting for nuclear decommissioning. For this material thickness, the cutting performance of the DOE plus the 250mm lens is as good as the 500mm lens alone, but the power density in the beam passing through the cut (which might illuminate something that should not be damaged), is approximately four times less when using the DOE and 250mm lens combination, compared to the 500mm lens alone. This is important if one considers the residual beam passing through the cut, impinging on say a concrete wall.

Figure 11 shows the effect on old concrete, of a 5kW laser beam from a 500mm lens (top) and from the DOE plus 250mm lens (bottom), both at a 1.5m distance between beam focus and concrete surface. In this case the travel speed (1.5m/min) was chosen so that the DOE and 250mm lens combination produced light enough damage to the surface to be seen. When using the 500mm lens (at the same speed), it is clear the induced damage is significantly greater and involves both scabbling and vitrification of the concrete surface to a few mm in depth.

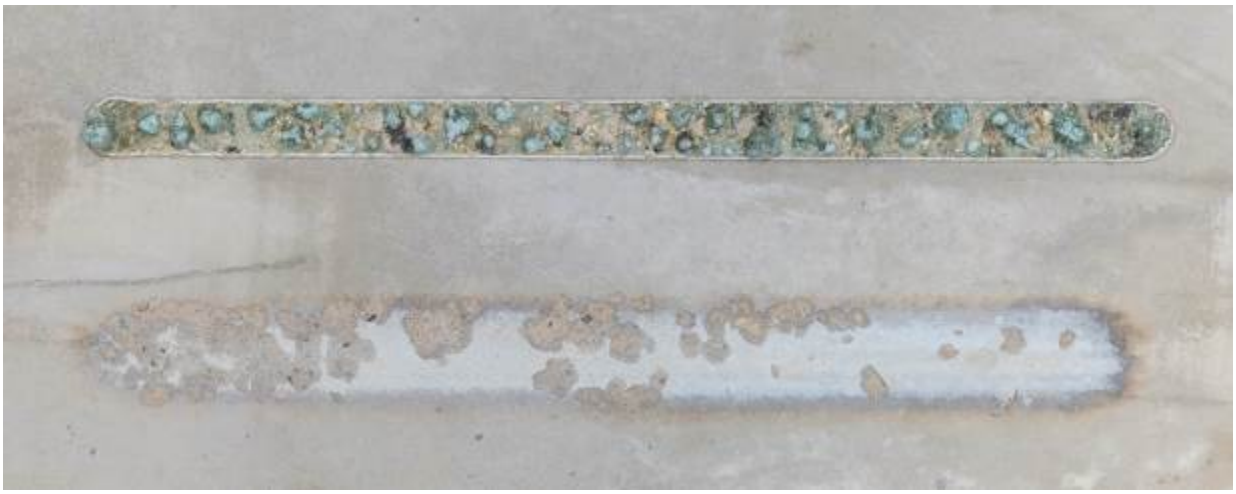

Figure 11. *Effect of residual laser beam on a concrete surface. 500mm lens (top), DOE plus 250mm lens (bottom), for the same laser power, beam focus to concrete distance and travel speed.*

The DOE/lens combination maintains the power density through an increased depth of field. The results in this work show the cutting process is not simply driven by laser power density at the beam waist as, from Table 1, this is lowest with the combination of the DOE and 250mm lens. The power density influences the temperature profile of the cutting front and the thickness of the melt front. This affects the distance of any

melted material to the nearest liquid free surface, which in turn, influences the width and temperature of the melt front development.

It can be seen from the heat affected zones revealed in the cross-sections of Figure 7, that both DOE/lens sections show a much narrower heat affected zone than the conventional cut sections. This might have potential benefits in terms of the material properties along the cut section, which have not been investigated here.

The energy distribution generated by the DOE in this work was omni-directional, like most laser beams used in materials processing. Use of DOE's to create more complex shapes could further allow increased cutting performance. However, this would result in the beam having a preferential cutting direction. Design of such shapes and especially their resolution, would need to account for the effects of multimode beams, as the edge quality of the beam will, in these cases, be noticeably reduced. This can however, be avoided by use of single mode laser systems, which are now available at (at least), the powers used in this work. The work reported here has shown the potential benefits of the use of DOE's in cutting, particularly for nuclear decommissioning applications. It would be useful to now seek further redistribution of the cutting profile, to further enhance performance, following modelling of the process. The DOE/lens combination offers an ideal combination to then implement such an optimised profile in real applications.

CONCLUSION

This work, using a laser power of 5kW for cutting C-Mn steel, has allowed the following conclusions to be made:

- A DOE has been designed and manufactured, which when used in conjunction with a conventional focusing lens, has been able to increase the beam waist diameter and the Rayleigh length of the focusing beam, whilst maintaining the 'focal length' of the lens alone.
- The DOE, even though it was not anti-reflection coated at 1µm, has been used at laser powers of up to 5kW for extended cutting experiments without apparent deterioration.
- In terms of cutting 40mm C-Mn steel plate, a DOE and 250mm lens combination has the same cutting performance, in terms of tolerance to stand-off distance and speed, as a 500mm lens alone.
- When using the DOE and lens combination, 40mm thick C-Mn steel was cut at a speed of 50mm/min, whilst the beam focus position was continuously cycled from a position 20mm below the plate surface to a position 80mm above the plate surface.
- The residual defocused laser beam, using the DOE and lens combination, has a power density approximately four times less than that when cutting with the 500mm lens alone.

REFERENCES

1 C Chagnot, G de Dinechin, G Canneau, and J-M Idasiak, 2009: 'Dismantling nuclear power plant with new industrial cw Nd:YAG high power lasers' Proceedings of Global, Paris, France, Sept, Paper 9539.

2 Hilton P A and Walters C L. 2010: 'The laser alternative in nuclear decommissioning - tube cutting and concrete scabbling using the latest technology'. Nuclear Engineering International, Vol 55, no 672.

3 Hilton P A, Khan A and Walters C L. 2010: 'The Potential of lasers in nuclear decommissioning'. ENC, European Nuclear Conference, Barcelona, Spain, 30 May - 2 June. European Nuclear Society.

4 Hilton P A and Khan A, 2012: 'Advances in laser cutting as a decommissioning and dismantling tool' ENC. European Nuclear Conference, Manchester, UK, June. European Nuclear Society.

5 Hilton P A, 2013: 'Parameter Tolerance Evaluation when Laser Cutting in Decommissioning Applications' Proc. ICALEO, Miami, paper 501. Laser Institute of America.

6 Khan A, Cruikshank H, Woodcock T, Pullin I and Silverwood S, 2015: 'Laser Size Reduction of Contaminated Magnox Pond Skips' – paper 15166 WM2015, Phoenix, Arizona.

7 Hilton P A, 2014: 'Towards a safety case for the use of laser cutting in nuclear decommissioning' ENC, European Nuclear Conference, Marseilles, France. European Nuclear Society.

8 Cole C E, Noden S C, Tyrer J R; Hilton P A, 1998: 'The application of diffractive optical elements in high power laser material processing'. Laser Materials Processing. Proc. Conf. ICALEO, Orlando, Florida Laser Institute of America. ISBN 0-912035-58-7. Vol.85. Part 1. Section A. pp84-93.

9 Goffin N J, Higginson, R L, Tyrer J R, The use of Holographic Optical Elements (HOE's) to investigate the use of a flat irradiance profile in the control of heat absorption in wire-fed laser cladding, Journal of Materials Processing Technology (2015), http://dx.doi.org/10.1016/j.jmatprotec.2015.01.023

10 Kell J, Tyrer J R, Higginson, R L, Jones, J C, Noden S, 2012. Laser weld pool management through diffractive holographic optics. Materials Science and Technology, 28(3)

11 Olsen F, 2011: Laser metal cutting with tailored beam patterns. Industrial Laser Solutions. September.

12 Noden S C, 2000, 'The application of diffractive optical elements in high power laser materials processing'. PhD Thesis, Loughborough University.

13 Dresel T, Beyerlein M, and Schwider J, 'Design and fabrication of computer-generated beam-shaping holograms,' Appl. Opt. 35, 4615-4621 (1996).

ACKNOWLEDGEMENTS

This work was carried out as part of the LaserSnake2 collaborative research project. LaserSnake2 is co-funded by Innovate UK, the Department of Energy and Climate Change, and the Nuclear Decommissioning Authority, under Grant number 110128. The LaserSnake2 project includes OC Robotics, TWI, Laser Optical Engineering, ULO Ltd and the UK's national Nuclear Laboratory.